# **Experimental and Computational Gas Phase Acidities of Conjugate** Acids of Triazolylidene Carbenes: Rationalizing Subtle Electronic **Effects**

Yijie Niu, †,§ Ning Wang, †,§ Alberto Muñoz,‡ Jiahui Xu,† Hao Zeng,† Tomislav Rovis,\*,‡ and Jeehiun K. Lee\*,†6

Department of Chemistry and Chemical Biology, Rutgers, The State University of New Jersey, New Brunswick, New Jersey 08901, United States

Supporting Information

ABSTRACT: In recent years, triazolylidene carbenes have come to the forefront as important organocatalysts for a wide range of reactions. The fundamental properties of these species, however, remain largely unknown. Herein, the gas phase acidities have been measured and calculated for a series of triazolium cations (the conjugate acids of the triazolylidene carbenes) that have not been heretofore examined in vacuo. The results are discussed in the context of these species as catalysts. We find correlations between the gas phase acidity and selectivity in two Umpolung reactions catalyzed by these species; such correlations are the first of their kind. We are able to use these linear correlations to improve reaction enantioselectivity. These results establish the possibility of using these thermochemical properties to predict reactivity in related transformations.

## ■ INTRODUCTION

Downloaded via RUTGERS UNIV on August 29, 2023 at 18:58:21 (UTC). See https://pubs.acs.org/sharingguidelines for options on how to legitimately share published articles.

Since the discovery of stable carbenes, first reported independently by Bertrand et al. and Arduengo et al., these species have become key players in organic and organometallic chemistry. 1,2 N-Heterocyclic carbenes (NHCs), particularly imidazolylidenes, have come to the forefront as effective ligands for transition-metal catalysts, with perhaps the best-known example being the Grubbs second-generation ruthenium catalysts for olefin metathesis.3 In addition to their role as key ligands for organometallic catalysts, NHCs themselves can also function as organocatalysts, and in recent years, triazolylidene carbenes have emerged as the most prominent structure. 4,5 Work in this field has encompassed both Umpolung and non-Umpolung reactions, with an eye to stereoselectivity.4-

For reactions catalyzed by triazolylidene carbenes, the carbene is often generated in situ by deprotonation of the corresponding triazolium precatalyst. The resultant carbene behaves as a nucleophile; for most reactions catalyzed by NHCs, the first step in the catalytic cycle is NHC attack of an electrophile. An example of an NHC-catalyzed reaction from our lab, the intramolecular Stetter reaction, is shown in Figure 1. Because of the requisite deprotonation of the precatalyst and the nucleophilic nature of the carbene, the acidity of the triazolium precatalyst (which is equivalent to the basicity of the free carbene) and the nucleophilicity of the triazolylidene carbene catalyst are of great interest.

Despite great progress in the development and optimization of triazolylidene carbenes as catalysts for enantioselective reactions, fundamental studies of these species are relatively limited. With respect to the evaluation of the acidity of these triazoliums, Smith, O'Donoghue, and co-workers conducted a seminal study that yielded the acidity of 20 triazolium salts in aqueous solution. 7,8 Mayr and co-workers examined a series of NHCs to evaluate nucleophilicity and Lewis basicity. They found that triazolylidene C is less nucleophilic than imidazolylidene A and imidazolinylidene B; all three had moderate nucleophilicity relative to a high Lewis basicity.

In this paper, we describe our studies of a series of triazolium cations that, upon deprotonation, deliver catalysts that are active

Received: May 20, 2017 Published: October 17, 2017

<sup>\*</sup>Department of Chemistry, Columbia University, New York, New York 10027, United States

$$R^{1} \xrightarrow{N \oplus N \oplus N - Ar} R^{2} \xrightarrow{N - Ar} R^{2$$

**Figure 1.** Intramolecular Stetter reaction cycle as catalyzed by a triazolylidene NHC.

in a variety of transformations. Herein we use experiment and theory to characterize the intrinsic basicity of triazolylidenes by measuring and computing the acidity of the corresponding triazolium cations in the gas phase, for a wide range of achiral and chiral species not heretofore examined in vacuo.

## RESULTS AND DISCUSSION

Achiral Pyrrolidine-Based Triazoliums. Calculations: Achiral Pyrrolidine-Based Triazolium Cations. We first studied a series of achiral pyrrolidine-based triazolium cations (Figure 2).

These compounds were chosen to assess the electronic effect of the various substituted phenyl moieties; also, the aqueous  $pK_a$ has been measured for some of these, which would allow us to compare gas and solution phase values. The calculated acidities of the triazolium cations, which correspond to the proton affinity of their respective triazolylidene carbenes, are listed in Figure 2. In our experience, density functional theory (DFT) methods generally yield accurate values for thermochemical properties of heterocyclic rings, so we utilized B3LYP/6-31+G(d) to calculate the acidities  $(\Delta H_{\rm acid})^{10-15}$  The overall trend in terms of acidity for these substrates is as follows (from most acidic to least acidic; note that as with  $pK_a$  values, more acidic species have lower  $\Delta H_{\text{acid}}$  values): 1c > 1b = 1e > 1g > 1f > 1i > 1h > 1a > 1l > 1d >1j > 1k. Overall, this trend makes sense: 1c is most acidic, with a 3,5-di-CF<sub>3</sub> substitution on the phenyl, followed by perfluorophenyl and 4-cyanophenyl. Ultimately the least acidic is 1k, with a largely electron donating N-aryl group substituent.

There is one surprise in this trend, however, which is the higher acidity of 1c (242.7 kcal/mol) versus 1g (248.0 kcal/mol). 1c has a phenyl ring with 3,5-di-CF<sub>3</sub> substitution while 1g has a

**Figure 2.** Calculated acidities for a series of pyrrolidine-based achiral triazolium cations (kcal/mol). Calculations were conducted at B3LYP/6-31+G(d); reported values are  $\Delta H$  at 298 K.

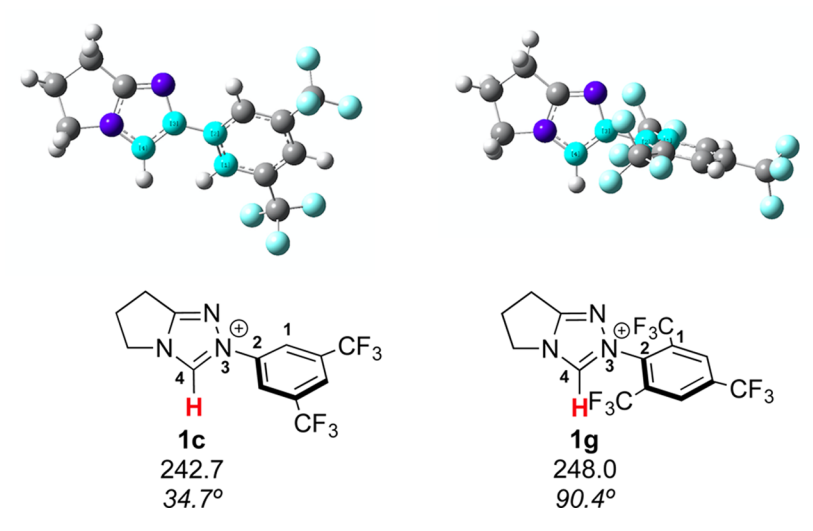


Figure 3. Calculated (B3LYP/6-31+G(d)) geometries of the 1c and 1g achiral triazolium cations.

Table 1. Summary of Results for Gas Phase Acidity Bracketing of Achiral Pyrrolidine-Based Triazoliums

		proton transfer to reference base $^d$									
reference base <sup>ab</sup>	PA (kcal/mol) <sup>c</sup>	1c	1b	1e	1f	1i	1h	1a	1d	11	1j
N,N,N',N' -tetramethylethylenediamine	242.1	_									
1-(cyclopent-1-en-1yl)pyrrolidine	243.6	_	_	_		_					
N,N,N',N'-tetramethyl-1,3-propanediamine	247.4	+	_	_		_	-	_			
DBN	248.2	+	+	+	-	_	-	_			
DBU	250.5	+	+	+	-	_	-	_	_	_	
MTBD	254.0				+	+	+	+	_	_	_
$HP_1(dma)$	257.4				+	+	+	+	+	+	_
$tBuP_1(dma)$	260.6								+	+	+
$tOctP_1(dma)$	262.0										+

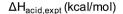
"Reference 16. bDBN = 1,5-Diazabicyclo[4.3.0]non-5-ene; DBU = 1,8-diazabicyclo[5.4.0]undec-7-ene; MTBD = 7-methyl-1,5,7-triazabicyclo[4.4.0]dec-5-ene; HP<sub>1</sub>(dma) = imino-tris(dimethylamino)phosphorane; tBuP<sub>1</sub>(dma) = tert-butylimino-tris(dimethylamino)phosphorane; tOctP<sub>1</sub>(dma) = tert-butylimino-tris(dimethylamino)phosphorane; tBuP = 2-tert-butylimino-2-diethylamino-1,3-dimethylperhydro-1,3,2-diazaphosphorine. Reference base PAs typically have an error of ±2 kcal/mol. The "+" symbol indicates the occurrence, and the "-" symbol indicates the absence of proton transfer.

phenyl ring with an additional trifluoromethyl group, as well as diortho substitution (2,4,6-tri-CF<sub>3</sub>). One might initially expect 1g to be more acidic than 1c, due to the additional electron withdrawing trifluoromethyl group. However, we suspected that the additional trifluoromethyl group (as well as the diortho substitution pattern) alters the phenyl ring geometry unfavorably, which calculations confirmed (Figure 3). For 1c, the phenyl ring is relatively planar relative to the triazolium ring; the dihedral angle for the calculated structure (for the atoms labeled 1-2-3-4) is 34.7°. For **1g**, however, the relatively bulky trifluoromethyl groups, placed at the ortho positions of the phenyl ring, cause the ring to become nearly perpendicular to the triazolium ring (dihedral 90.4°). A perpendicular disposition of the aryl ring leads to reduced orbital overlap with the azolium and a minimization of its impact on the electronic character of the carbene center. Therefore, although the additional trifluoromethyl would be expected to increase the acidity, the lack of planarity of the phenyl ring relative to the triazolium core mitigates the effect of the third CF<sub>3</sub>. This is reminiscent of the surprisingly similar acidities of diphenylmethane and triphenylmethane; the third phenyl ring is less effective than might be expected due to the inability of all three phenyl rings to be in the same plane.

To avoid this type of complication when looking at trends, a more reasonable comparison is to focus on structures that have the same substitution pattern. For example, among the 2,4,6-substituted phenyl compounds, the order from most to least acidic is  $\mathbf{1g}$  (2,4,6-tri-CF<sub>3</sub>) >  $\mathbf{1i}$  (2,4,6-tri-Cl) >  $\mathbf{1h}$  (2,4,6-tri-Br) >  $\mathbf{1j}$  (2,4,6-tri-CH<sub>3</sub>(mesityl)) >  $\mathbf{1k}$  (2,4,6-tri-OCH<sub>3</sub>). In terms of electron withdrawing capability, this trend is reasonable: the most acidic is the compound with the 2,4,6-tri-CF<sub>3</sub>-phenyl moiety and the least acidic has a 2,4,6-tri-OCH<sub>3</sub>-phenyl group. For the 4-substituted phenyls, the acidity order is (from most to least acidic):  $\mathbf{1e}$  (4-CN) >  $\mathbf{1f}$  (4-F) >  $\mathbf{1d}$  (4-OMe), which also makes sense.

Experiments: Achiral Pyrrolidine-Based Triazolium Cations. To experimentally measure the gas phase acidity of the achiral triazolium cations, we utilized mass spectrometry and proton transfer reactions between the protonated carbene precursors and various bases in the gas phase whose proton affinities are known. Electrospray ionization of the protonated carbene successfully yields the triazolium cation as the major signal. Reference bases are then added and the presence or absence of proton transfer is assessed.

DBU (PA = 250.5 kcal/mol) is unable to deprotonate 1a, but MTBD (PA = 254.0 kcal/mol) can. We therefore bracket the acidity of 1a to be between DBU and MTBD (252  $\pm$  4 kcal/



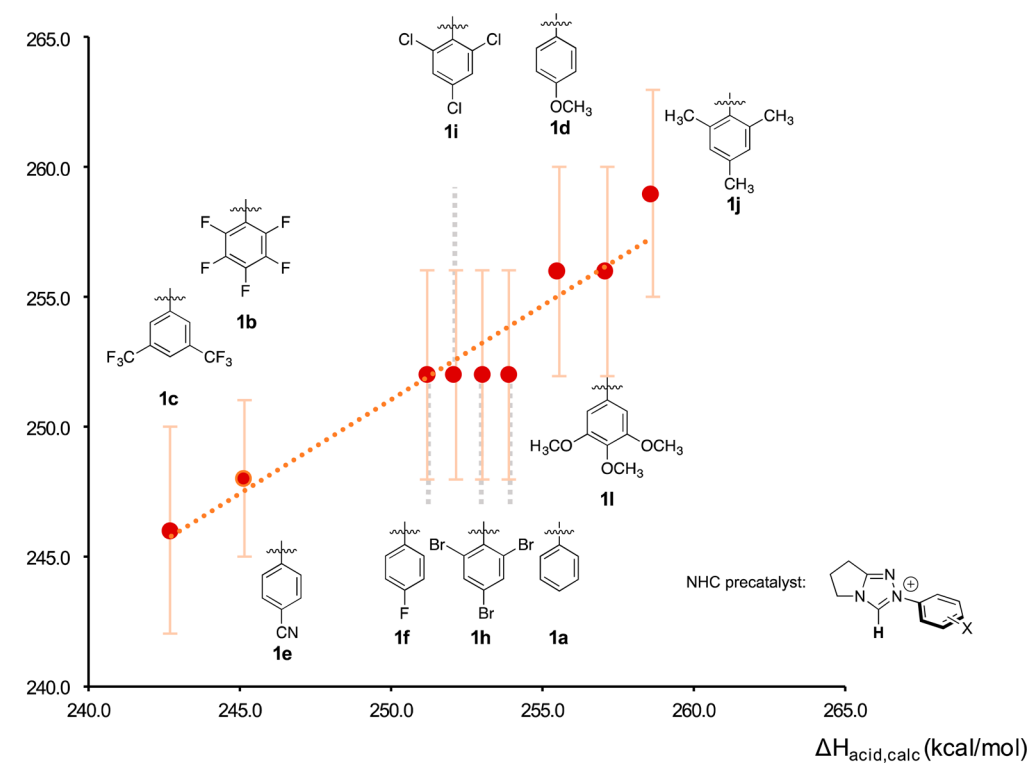


Figure 4. Plot of experimental versus calculated acidity for compounds 1.

Table 2. Calculated (B3LYP/6-31+G(d); 298 K) Gas Phase Acidity and pK<sub>a</sub> Values for Achiral Triazolium Cations<sup>a</sup>

substrate	calcd $\Delta H_{ m acid}$	calcd $\Delta G_{ m acid}$	$pK_a^{b}$						
1c	242.7	235.0							
1b	245.1	237.4	16.5						
1e	245.1	237.6	16.9						
1g	248.0	240.9							
1f	251.2	243.5	17.4						
1i	252.1	244.5							
1h	253.0	245.4							
1a	253.9	246.3	17.5						
11	255.5	248.1							
1d	257.1	249.4	17.8						
1j	258.6	250.7	17.7						
1k	267.5	260.0							
$^a\Delta H_{\rm acid}$ and $\Delta G_{\rm acid}$ values are in kcal/mol. $^b$ Reference 7.									

mol). For 1b, as well as 1e, N,N,N',N'-tetramethyl-1,3propanediamine (PA = 247.4 kcal/mol) is unable to effect deprotonation, but DBN (PA = 248.2 kcal/mol) can, placing the acidity of 1b and 1e at 248 ± 3 kcal/mol. 1-(Cyclopent-1-en-(PA = 243.6 kcal/mol) cannot deprotonate 1c, kcal/mol) can; we therefore bracket the acidity of 1c to be 246  $\pm$ 4 kcal/mol. For 1d, no reaction is observed with MTBD (PA = 254.0 kcal/mol), but proton transfer occurs with  $HP_1(dma)$  (PA = 257.4 kcal/mol), placing the acidity of 1d at 256  $\pm$  4 kcal/mol. For 1f, 1h, and 1i, no proton transfer is observed with DBU (PA = 250.5 kcal/mol) but MTBD (PA = 254.0 kcal/mol) deprotonates all three, allowing us to bracket the acidity of 1f, 1h, and 1i to be the same,  $252 \pm 4 \text{ kcal/mol}$ . 1j is least acidic;  $HP_1(dma)$  (PA = 257.4) cannot deprotonate it, but  $tBuP_1(dma)$ 

(PA = 260.6) can, bracketing the acidity of 1j to 259  $\pm$  4 kcal/ mol. MTBD (PA = 254.0 kcal/mol) does not deprotonate 1l, but  $HP_1(dma)$  (PA = 257.4 kcal/mol) does, placing the acidity of 11 at  $256 \pm 4 \text{ kcal/mol}$ .

The overall trend for the experimental acidity values tracks reasonably well with calculation (from most acidic to least acidic): 1c > 1b = 1e > 1a = 1f = 1h = 1i > 1d = 1l > 1j (Table 1 and Figure 4). Reference bases are limited in this region, which is at the high basicity range for compounds in the gas phase. Therefore, although calculations indicate that 1a, 1f, 1h, and 1i have different acidities (ranging from about 251–254 kcal/mol), all four substrates have a measured acidity of  $252 \pm 4$  kcal/mol. There are simply not enough reference bases to differentiate within this region. However, the calculations and experiments are in agreement, within the experimental uncertainty.

The aqueous  $pK_a$  values for some of these achiral triazoliums have been determined.<sup>7</sup> In Table 2, we list our calculated gas phase acidity values ( $\Delta H_{\rm acid}$  and  $\Delta G_{\rm acid}$ ) as well as known p $K_{\rm a}$ values. The data in Table 2 is arranged in order of decreasing calculated gas phase acidity.<sup>17</sup> The aqueous acidity trend, in a general sense, reflects the gas phase trend, meaning, as one moves down the table, the acidity generally decreases for both the gas phase and solution. The acidity range, however, is much greater in the gas phase than in solution. The range of gas phase acidities for those cations for which we have solution phase data is more than 13 kcal/mol, whereas the p $K_a$  range is less than 2 kcal/mol. In addition to a tighter range, some of the  $pK_a$  values do not exactly correlate to the gas phase values; gas phase calculations predict the same gas phase acidity for 1b and 1e, but in water 1e is less acidic than 1b by  $0.4 \, pK_a$  units. Also, calculations predict that 1d is more acidic than 1j, by 1.5 kcal/mol in the gas phase. In water, 1d is less acidic than 1j by 0.1 p $K_a$  units.

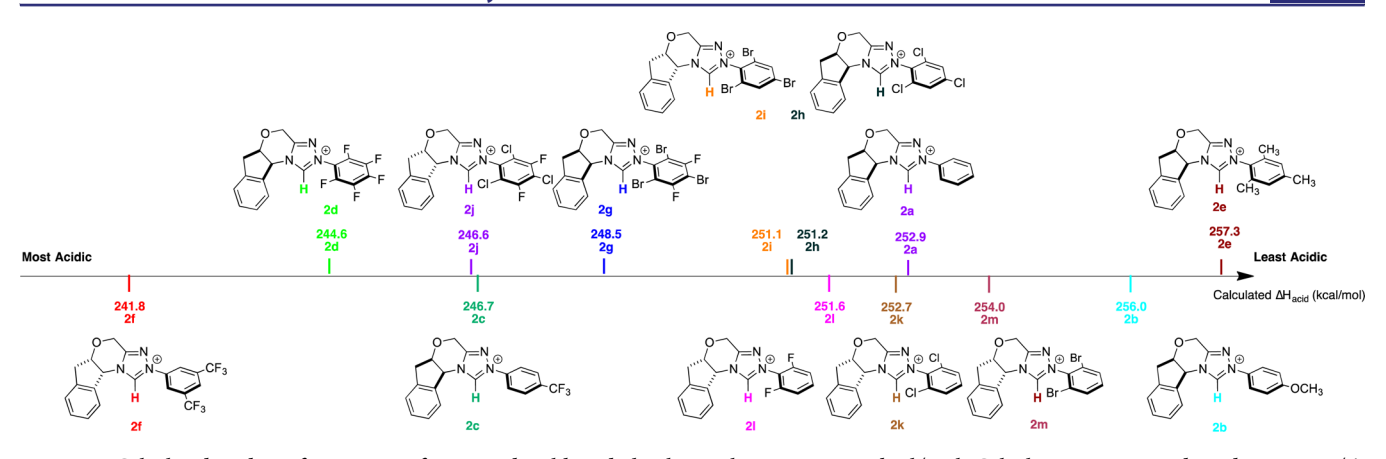


Figure 5. Calculated acidities for a series of aminoindanol-based chiral triazolium cations, in kcal/mol. Calculations were conducted at B3LYP/6-31+G(d); reported values are  $\Delta H$  at 298 K.

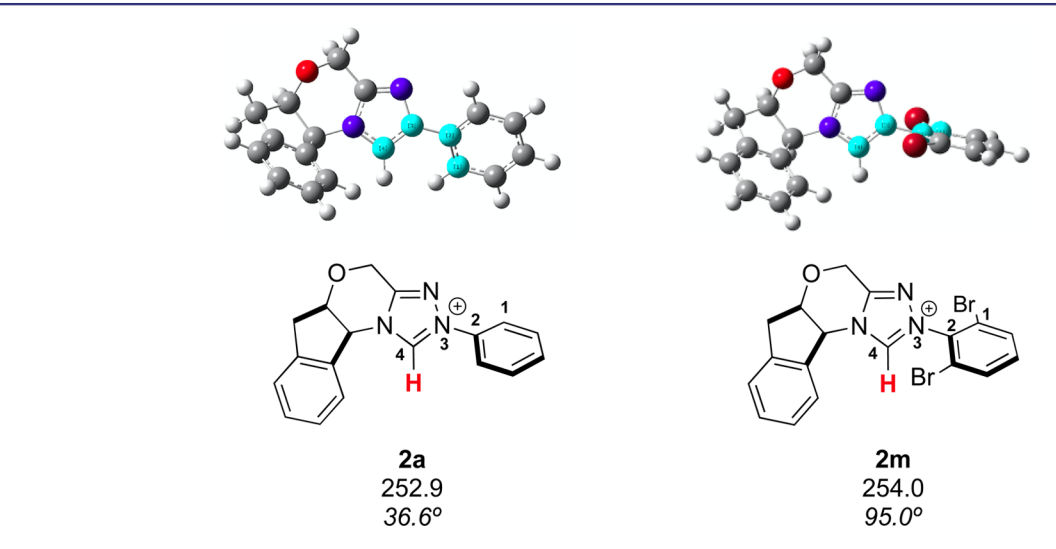


Figure 6. Calculated (B3LYP/6-31+G(d)) geometries of the 1a and 1m chiral triazolium cations.

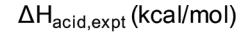
Table 3. Summary of Results for Acidity Bracketing of Chiral Aminoindanol-Based Triazolium 2a-2m

		proton transfer to reference base $^d$												
reference base ab	PA (kcal/mol) <sup>c</sup>	2f	2d	2j	2c	2g	2i	2h	21	2k	2a	2m	2b	2e
TMEDA	242.1	_	_											
1-CP	243.6	_	_	_	_	_		_				_	_	
TMPDA	247.4	+	_	_	_	_	_	_	_			_	_	
DBN	248.2	+	+	+	+	_	_	_	_	_	_	_	_	
DBU	250.5	+	+	+	+	+	+	+	+	_	_	_	_	_
MTBD	254.0		+	+	+	+	+	+	+	+	+	+	_	_
$HP_1(dma)$	257.4			+		+	+		+	+	+	+	+	_
$tBuP_1(dma)$	260.6										+		+	+
$tOctP_1(dma)$	262.0										+			+
BEMP	263.8										+			+

"Reference 16. "TMEDA = N,N,N',N'-Tetramethylenediamine; 1-CP = 1-(cyclopent-1-en-1yl)pyrrolidine; TMPDA = N,N,N',N'-tetramethyl-1,3-propanediamine; DBN = 1,5-diazabicyclo[4.3.0]non-5-ene; DBU = 1,8-diazabicyclo[5.4.0]undec-7-ene; MTBD = 7-methyl-1,5,7-triazabicyclo[4.4.0]dec-5-ene; HP<sub>1</sub>(dma) = imino-tris(dimethylamino)phosphorane; tBuP<sub>1</sub>(dma) = tert-butylimino-tris(dimethylamino)phosphorane; tOctP<sub>1</sub>(dma) = tert-octylimino-tris(dimethylamino)phosphorane; BEMP = tert-butylimino-2-diethylamino-1,3-dimethylamino-1,3,2-diazaphosphorine. "Reference base PAs typically have an error of tert2 kcal/mol. "The "+" symbol indicates the occurrence, and the "-" symbol indicates the absence of proton transfer.

The differences between gas phase and aqueous solution are attributable, generally, to solvent effects. It is well-known that acidity trends sometimes differ in the gas versus solution phases; the classic case is that *tert*-butanol is more acidic than methanol in the gas phase, while the opposite is true in water. <sup>18</sup> In the gas

phase, the polarizable methyl groups in *tert*-butoxide stabilize the anion; this is less keenly felt in solution, and also, water molecules may more poorly solvate the bulkier *tert*-butyl group. For our substrates, the gas phase results indicate that perfluoro and 4-CN phenyl moieties in **1b** and **1e**, respectively, have similar intrinsic



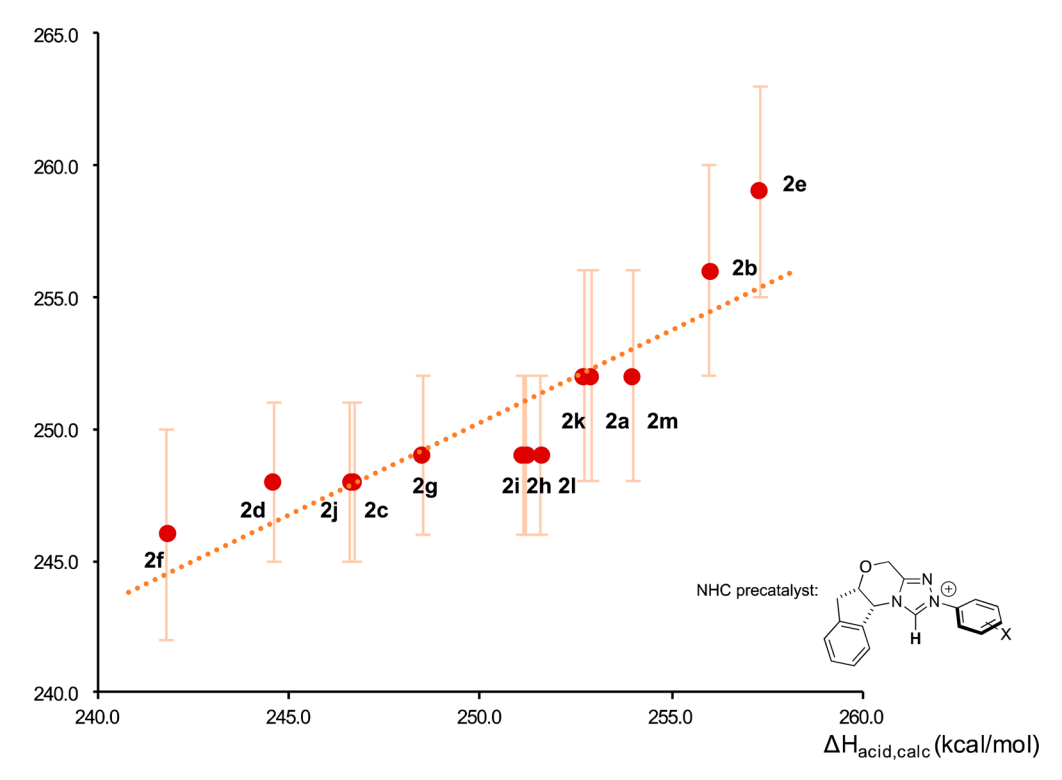


Figure 7. Plot of experimental versus calculated acidity for compounds 2.

anion stabilizing ability. With solvation, however, the polarizability of the cyano group may have less of an influence, causing 1e to be slightly less acidic than 1b. It is more difficult to make conclusions about 1d and 1j; they only differ by 1.5 kcal/mol in the gas phase, and therefore have a mere  $0.1 pK_a$  unit difference in solution (0.14 kcal/mol), due to the tighter range.

Last, the wider range of acidity for the catalysts in the gas phase also implies that differences in reactivity of catalysts will be more pronounced in nonpolar environments. Thus, for example, using a less polar solvent will allow for nuances among catalyst reactivity to stand out. Also, less solvent interference can increase catalyst efficacy; recent work by Kimura and co-workers using NHCs in solvent-free benzoin and Stetter reactions indicated efficient reactions with low catalyst loading. 19

Chiral Aminoindanol-Based Triazoliums. Calculations: Chiral Triazolium Cations. We also studied a series of chiral aminoindanol-based triazoliums that over the years have been used as precatalysts for a wide range of reactions.<sup>4-6</sup> The calculated acidities ( $\Delta H_{acid}$ ) of the triazolium cations are shown in Figure 5. The overall trend from most to least acidic, in the gas phase, is  $2f > 2d > 2j = 2c > 2g > 2i = 2h \ge 2l > 2k = 2a > 2m > 2b$ > 2e. As with the achiral triazoliums, the overall trend in acidity seems reasonable, with the most acidic species being the 3,5bis(trifluoromethylphenyl) and the least being the mesitylsubstituted catalyst. One perhaps surprising ordering is 2a versus 2m; the aminoindanol triazolium with an unsubstituted phenyl is more acidic than that with a 2,6-dibromo substituted phenyl. As with the achiral series, however, we find that the dihedral angle for 2a indicates a nearly flat phenyl ring (36.6°), whereas for 2m the dibromophenyl substituent is perpendicular (95.0°) to the triazolium ring. Presumably that perpendicularity will mean less of an electronic influence on the carbene center basicity (triazolium acidity) (Figure 6).

A comparison between achiral and chiral triazoliums and phenyl substitution also shows consistency in terms of the influence of the phenyl ring substitution on the triazolium carbene center acidity. Both series have a 3,5-bis-(trifluoromethylphenyl) substituent that renders the triazolium to be the most acidic of their respective groups (1c and 2f). This is followed by the perfluorophenyl substituted triazoliums and the 1,3,5-trihalophenyl substituted species, for both the  ${\bf 1}$  and  ${\bf 2}$ series. The acidity trend then continues for both series with an unsubstituted phenyl followed by 4-OMe then mesityl.

Experiments: Chiral Triazolium Cations. The experimental bracketing for the 2 series are shown in Table 3. DBU (PA = 250.5 kcal/mol) cannot deprotonate 2a but MTBD (PA = 254.0

Figure 8. NHC-catalyzed homoenolate addition of enals to nitroalkenes, with proposed catalytic mechanism.

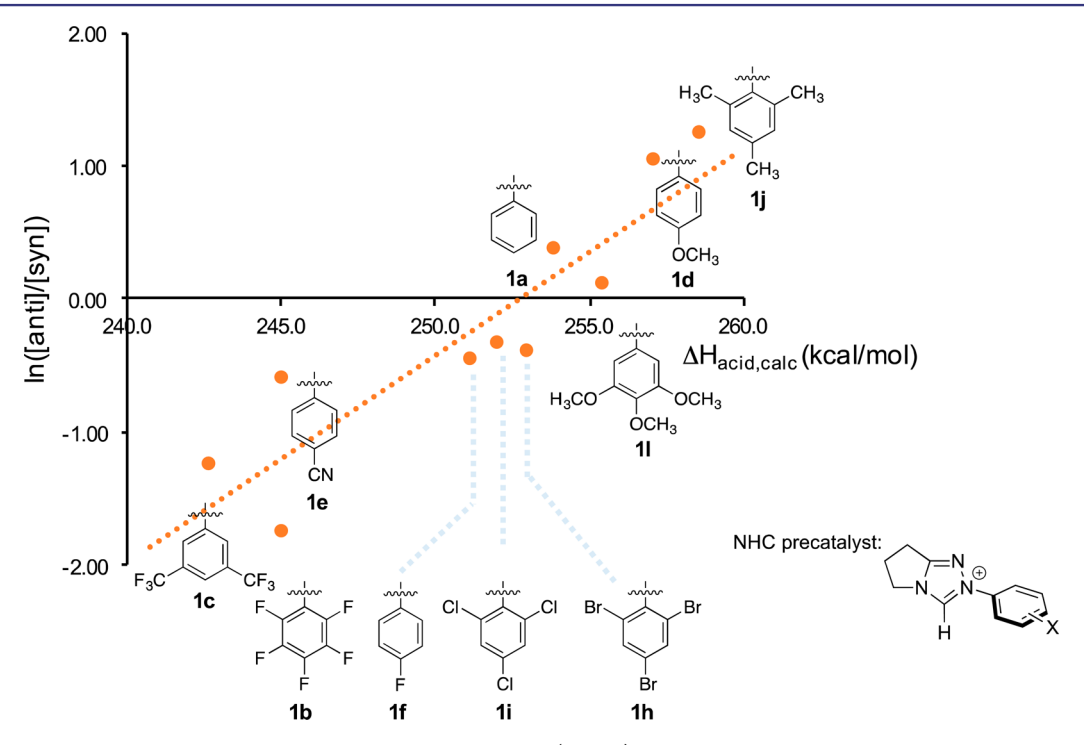


Figure 9. Natural log plot of the anti/syn ratio for the reaction in Figure 8 (R = Et) versus calculated gas phase acidity of the precatalyst.

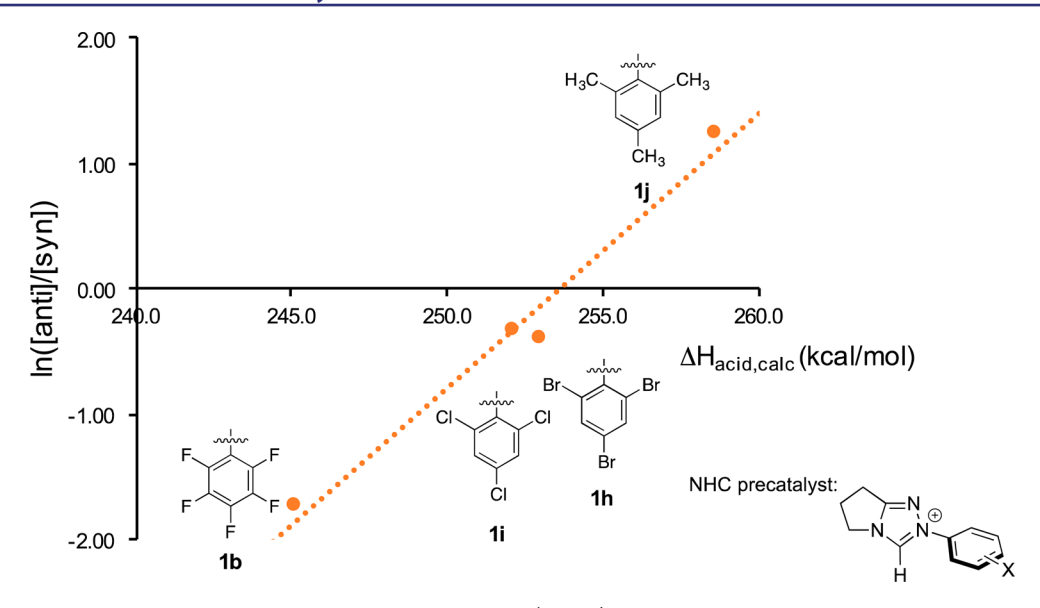


Figure 10. Natural log plot of the anti/syn ratio for the reaction in Figure 8 (R = Et) versus calculated gas phase acidity of the precatalyst, for catalysts with diortho aryl substitution.

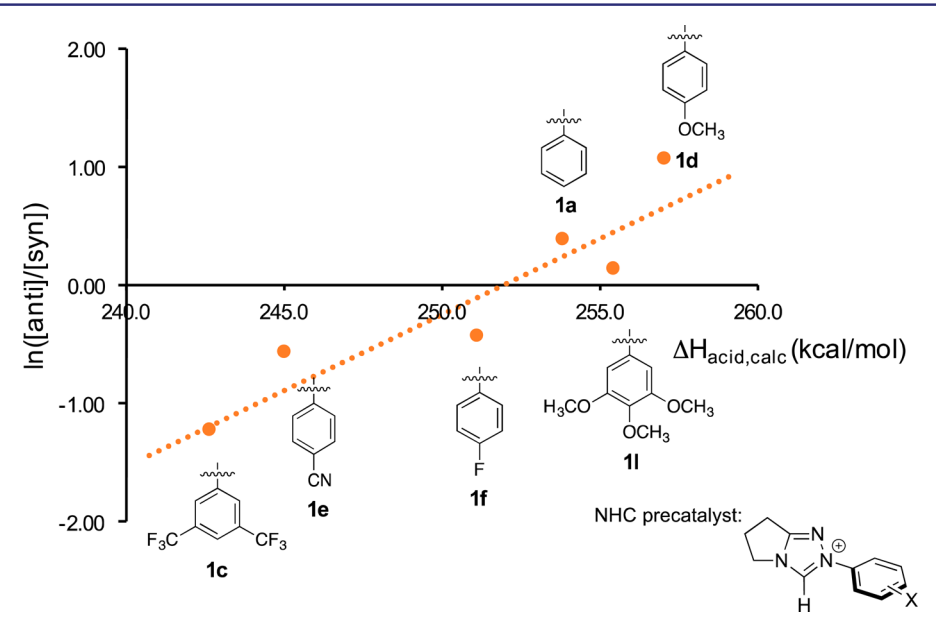


Figure 11. Natural log plot of the anti/syn ratio for the reaction in Figure 8 (R = Et) versus calculated gas phase acidity of the precatalyst, for precatalysts lacking diortho aryl substitution.

kcal/mol) can, placing the acidity of 2a at 252  $\pm$  4 kcal/mol. Triazoliums 2k and 2m bracket to the same acidity. For 2b, MTBD (PA = 254.0 kcal/mol) cannot deprotonate the triazolium but HP<sub>1</sub>(dma) (PA = 257.4 kcal/mol) can, which allows us to bracket the acidity of 2b to be  $256 \pm 4$  kcal/mol. We find that N,N,N',N'-tetramethyl-1,3-propanediamine (PA = 247.4 kcal/mol) is unable to effect deprotonation of 2c, but DBN (PA = 248.2 kcal/mol) can, placing the acidity of at  $248 \pm 3$ kcal/mol. Triazoliums 2d and 2j bracket to 248 kcal/mol as well. For 2e, HP<sub>1</sub>(dma) (PA = 257 kcal/mol) cannot effect deprotonation but tBuP<sub>1</sub>(dma) (PA = 260.6 kcal/mol) does, placing the acidity of **2e** at  $259 \pm 4 \,\text{kcal/mol}$ . 1-(Cyclopent-1-en-1-yl)pyrrolidine (PA = 243.6 kcal/mol) cannot deprotonate 2f but  $N_1N_2N_3N_3N_4$ -tetramethyl-1,3-propanediamine (PA = 247.4 kcal/mol) can, which gives an acidity of 246  $\pm$  4 kcal/mol. Last, DBN (PA = 248.2 kcal/mol) cannot deprotonate **2g**, but DBU

(PA = 250.5 kcal/mol) can. We thus bracket 2g to be 249  $\pm$  3 kcal/mol; substrates 2h, 2i, and 2l have the same acidity.

The computed and experimental gas phase acidity values for the chiral triazoliums are plotted in Figure 7. The experimental gas phase acidities roughly track with the calculated values. Given the small number of available reference bases in this superbasic range, it is not surprising that some of the experimental values are not exactly the same as the calculated values, though all are within error. Taken together, the achiral and chiral experimental data benchmark B3LYP/6-31+G(d) as a reasonable method and level to calculate the triazolium acidities.

**Acidity and Diastereoselectivity.** To further explore the relationship between the acidity of triazoliums 1 and reactivity, we explored the NHC-catalyzed homoenolate addition of cinnamaldehyde to nitroalkenes, shown in Figure 8. 20–22

This reaction has two potential products, anti and syn (one enantiomer of each is shown in Figure 8, but this racemic reaction

Figure 12. Transition states leading to the observed major isomers in asymmetric homoenolate reactions.

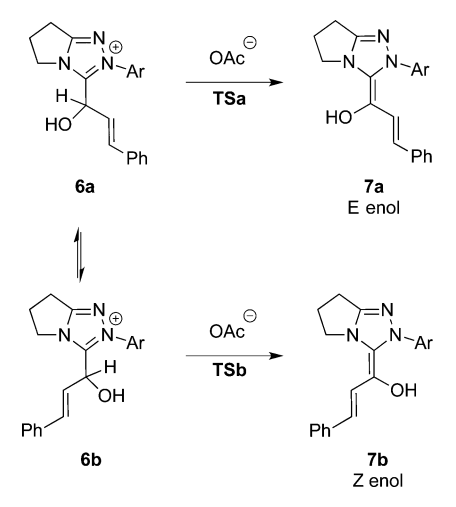


Figure 13. Deprotonation to form either E- or Z-enol.

yields both enantiomers for anti and for syn). An examination of the anti versus syn preference reveals a correlation to gas phase acidity. Figure 9 shows a plot of the natural log of the ratio of the anti to syn products versus the calculated acidity, for the reaction with (E)-1-nitrobut-1-ene. A correlation is observable, wherein a more acidic triazolium precatalyst corresponds to more syn product, and conversely, decreasing acidity correlates to increasing anti selectivity.  $^{23}$ 

While there is a clear overall trend, one pair of data points stands out: **1b** and **1e**. Both of these precatalysts have the same acidity (245.1 kcal/mol); however, they have different anti/syn selectivity, with 4-CN precatalyst **1e** showing more anti selectivity than the perfluorinated precatalyst **1b**. We suspect this difference is related to the substitution pattern for the two

precatalysts. The *N*-aryl group on **1b** has diortho substitution, while **1e** does not. Therefore, we also composed separate analyses, one with precatalysts that have diortho substituents and one with precatalysts that do not (Figures 10 and 11); these plots show the same trend (more acidic, more syn selectivity), but with slightly better correlations. In a study with this same class of catalysts, for the benzoin and Stetter reactions, O'Donoghue, Smith and co-workers proposed that perpendicularity of the *N*-aryl group, which should be greater with diortho substitution, influences reactivity. Our calculations do indicate that the catalysts with diortho substitution examined herein adopt geometries with a more perpendicular *N*-aryl group, which we assume influences the selectivity slightly differently than those catalysts without diortho substituents, which are less nonplanar.

We hypothesize, based on prior results, that the provenance of this linear correlation may lie in the acidity reflecting a preference for the E versus Z Breslow enol geometry. This type of reaction was first reported by Nair, using imidazolium precatalyst 3, which yielded the anti product as the major diastereomer. Enantioselective variations, using chiral triazolium precatalysts, were reported by the Rovis and Liu groups, respectively, in 2013 and 2012. Liu's precatalyst, 4, favors the anti isomer, while Rovis' precatalyst 5 favors the syn isomer. The difference in diastereoselectivity is proposed to arise from a difference in the Breslow intermediate geometry. Because the two chiral precatalysts 4 and 5 only allow approach from one face, the observed stereochemistry can be explained by E versus E Breslow enol geometry (Figure 12).

Applying what we learned from these chiral catalysts to our achiral system, we postulate that anti selectivity corresponds to a preference for the *E*-enol, while syn selectivity arises from a preference for the *Z*-enol. To further probe this hypothesis, we calculated the transition states for the formation of the *E*- and *Z*-

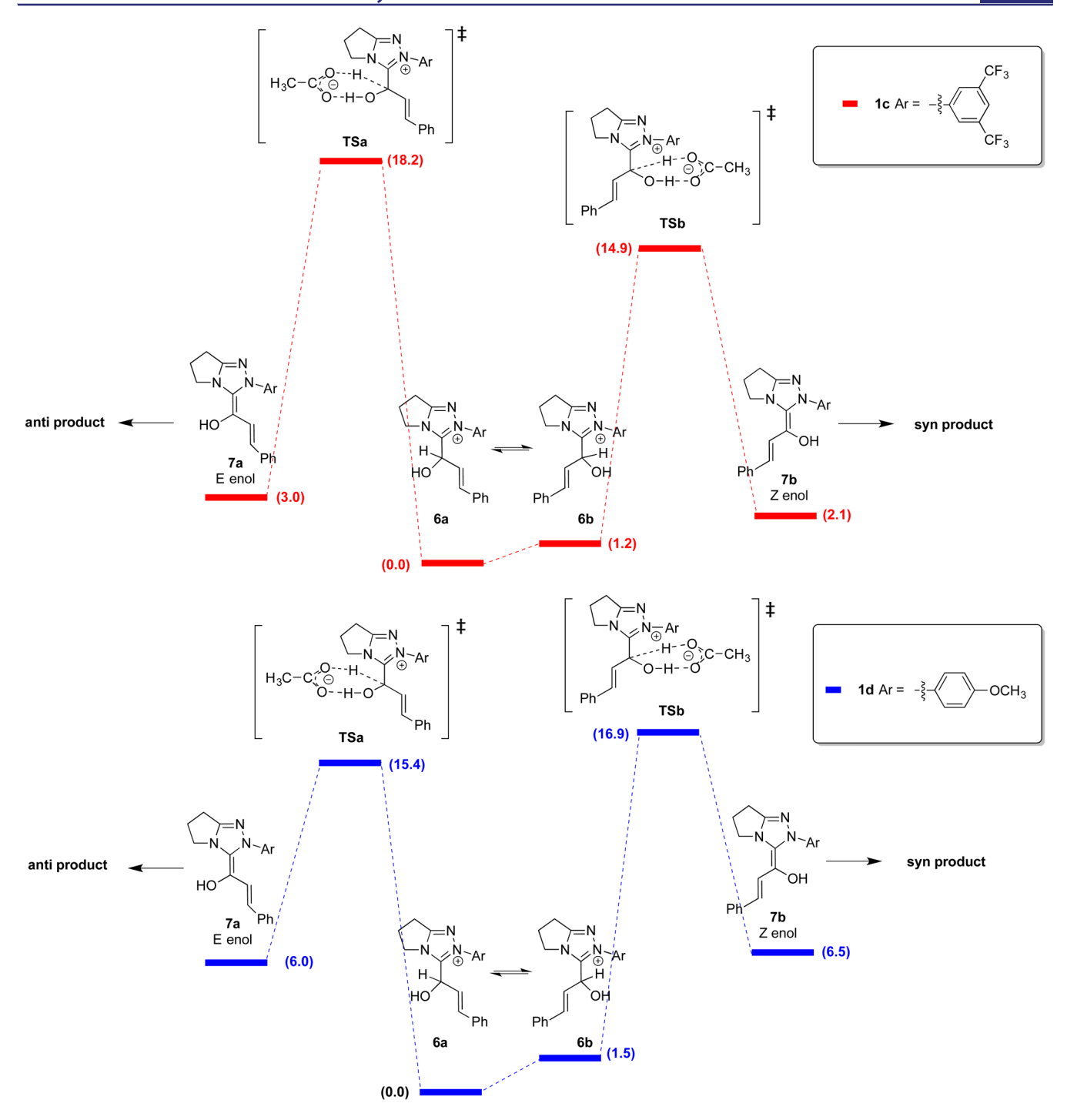


Figure 14. Free energy profiles for E- versus Z-enol formation for 1c and 1d.

enols via deprotonation by acetate (Figure 13). Intermediate 6a is deprotonated by acetate, via  $\mathbf{TSa}$ , to form the E-enol 7a; intermediate 6b reacts via  $\mathbf{TSb}$  to form Z-enol 7b. We examined 1c, which represents a highly acidic triazolium and 1d, a much less acidic triazolium. Both lack diortho substituents as well. For 1c (Ar = 3,5-di- $CF_3$ ), experimentally, we see syn selectivity (Figure 9). Our calculations show that for 1c, the transition state to form the Z-enol (TSb) is *lower* than that to form the E-enol (TSa) by 3.3 kcal/mol (Figure 14). This is consistent with our hypothesis that syn selectivity arises from the Z-enol. For 1d (Ar = 4-OMe), we find that the transition state for Z-enol formation is *higher* than that for E-enol formation, by 1.5 kcal/mol (Figure

14). This reversal, as compared to 1c, is consistent with the anti selectivity we experimentally observe for catalyst 1d.

We are not certain why electron withdrawing groups would favor Z-enol formation. An examination of the calculated geometries for the transition state leading to the Z-enol (TSb) indicates that TSb might be stabilized by an interaction between the enol oxygen and the N-aryl substituent (Figure 15). This interaction would be more favorable for an electron deficient ring; we find that the vertical distance between the enol oxygen and the plane defined by the N-aryl ring (point-to-plane distance) is indeed less for 1c (2.23 Å) than for 1d (2.39 Å), indicating a possibly stronger interaction.

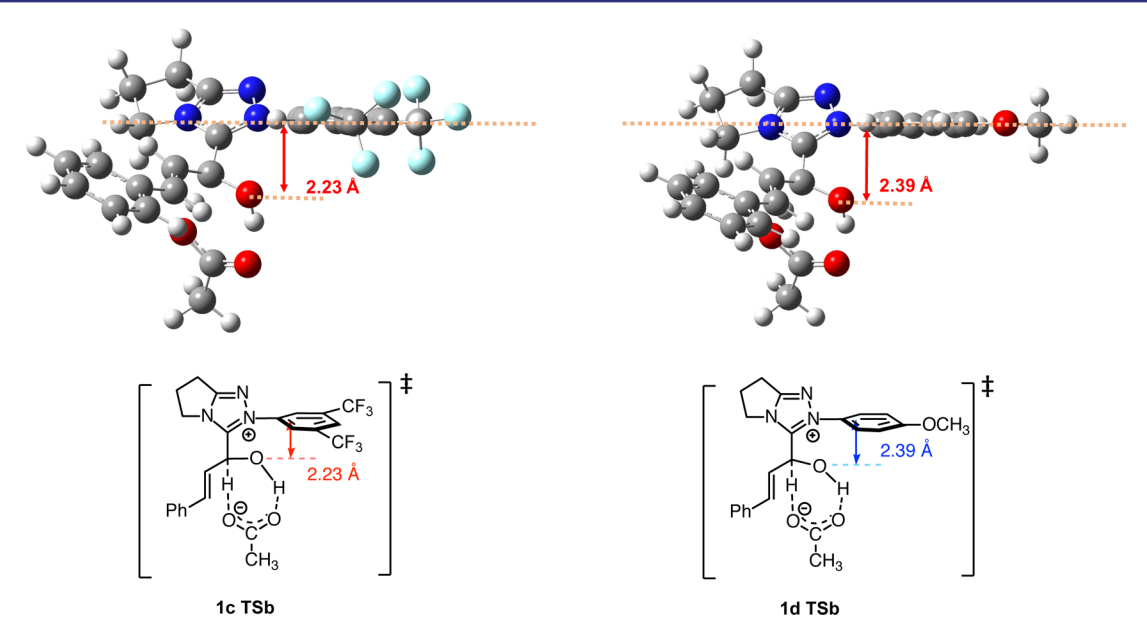


Figure 15. Calculated TSb structures for 1c and 1d.

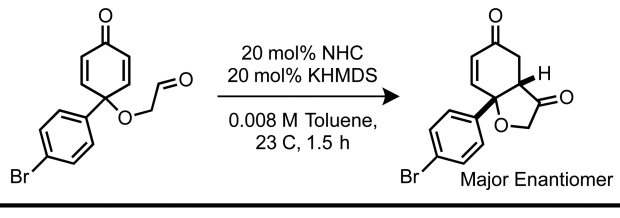


Figure 16. NHC-catalyzed intramolecular Stetter reaction with dienones.

In order to assess the generalizability of this result, we also examined the more acidic triazolium **1b**, as well as the less acidic triazolium **1j**; these contain diortho substituents. We find the same pattern as we report above for **1c** and **1d**; the more acidic **1b** favors the formation of the *Z*-enol and the syn product, and also has a smaller enol oxygen to aryl plane distance. These results can be found in the Supporting Information.

The postulate that the E-enol leads to anti selectivity and the Z-enol to syn selectivity is also consistent with calculations conducted by Fu and co-workers on precatalyst 5, which shows syn selectivity. <sup>25a</sup> Their computations indicate that, for 5, the Z-enol is afforded via a lower energy transition state relative to the E-enol, consistent with the syn selectivity that 5 presents.

Thus, these linear correlations show that gas phase acidity could be a potentially useful tool for improving on reaction selectivities for these types of transformations. Because gas phase acidities have a wider range than solution phase acidities, trends and correlations are easier to ascertain. We hypothesize, based on prior results, that the provenance of the correlation lies in the acidity reflecting a preference for the *E* versus *Z* Breslow enol geometry; current calculations are in agreement with this

hypothesis, and studies are currently underway to delve more deeply into this.  $^{20-22}$ 

**Acidity and Enantioselectivity.** To explore whether a correlation between acidity and enantioselectivity exists for reactions catalyzed by chiral triazolylidenes **2**, we examined an NHC-catalyzed asymmetric intramolecular Stetter reaction (Figure 16).<sup>26</sup>

An examination of the stereochemical outcome of this reaction reveals a linear correlation for the natural log of the ratio of major to minor enantiomer products versus the gas phase acidity of triazolium precatalysts 2 (Figure 17).<sup>27</sup> For this reaction, a more acidic triazolium corresponds to reduced enantioselectivities and a less acidic triazolium results in higher enantiomeric excesses.

This correlation with acidity also allowed us to improve the ee of this reaction. The previous ee benchmark for this particular substrate and for the antipode of precatalyst **2b** was an acceptable 73%. Realizing that a precatalyst with a lower gas phase acidity should improve enantioselectivity, we examined precatalyst *ent*-**2e**, resulting in 90% ee, exceeding our previous benchmark for this substrate by 17% (~0.6 kcal/mol at ambient temperature; new benchmark in red in Figure 17). Thus, calculated and experimental acidities may aid in a more rational catalyst optimization for *Umpolung*-themed reactions.

We postulate that the correlation between acidity and enantioselectivity for this reaction may be related to a bimolecular event in the mechanism. In a previous study of this reaction, we found that when using a solvent mixture of toluene and isopropanol, increasing the concentration of the alcohol decreased the ee.<sup>28</sup> We proposed that the alcohol is involved in the transition state structure via hydrogen bonding, either to the Breslow enol oxygen or the dienone carbonyl, or both. In the absence of alcohol, another species could provide the hydrogen bonding. Since more hydrogen bonding decreases the ee, then it should follow that a more acidic Breslow enol would favor hydrogen bonding, and decrease the ee. More electron withdrawing aryl substituents should increase the acidity of the precatalyst as well as the acidity of the Breslow intermediate. Thus, we see the correlation in Figure 17, between higher acidity and lower ee. Further studies to pinpoint the provenance of the linear correlation are currently underway.

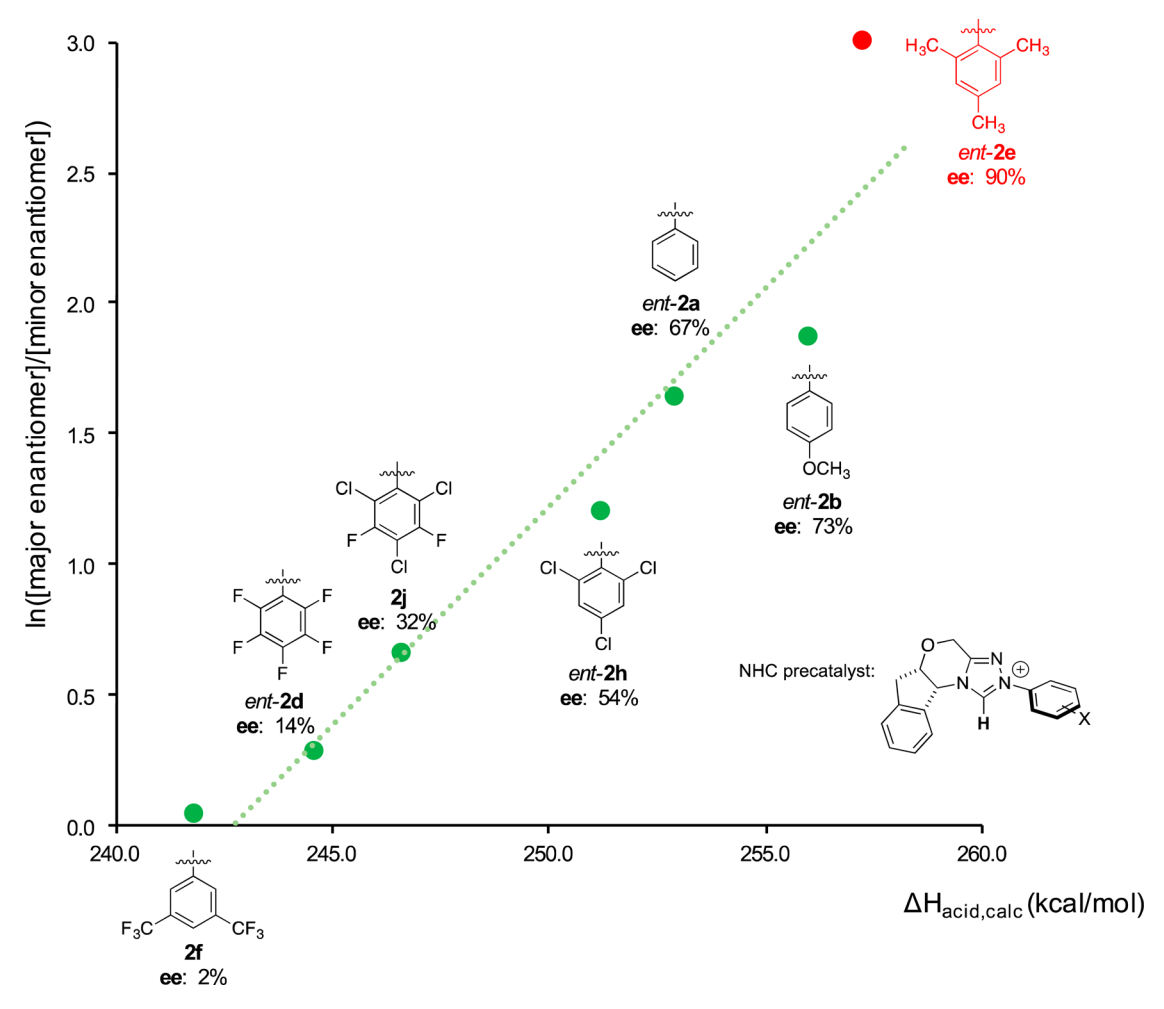


Figure 17. Natural log plot of the major/minor enantiomer ratio for the reaction in Figure 16 versus the calculated gas phase acidity of the precatalyst.

Our achiral and chiral selectivity studies, taken together, indicate that using gas phase acidity is a powerful and simple method to assess intrinsic properties of carbenes that can thus provide the backbone for predictive models for Umpolungthemed reactions. The nonpolar environment of the gas phase enhances the differences among acidities, making acidity trends clear. These acidity trends are found to correlate with selectivity, a novel finding. Solution phase acidities should also correlate to selectivity, but are generally more difficult to obtain<sup>7,8,29-35</sup> furthermore, it is potentially more difficult to ascertain acidity trends among  $pK_a$  values since the overall acidity range, as we show herein, is much tighter in solvent than in the gas phase. Gas phase acidity calculations are easily obtained, and the experimental measurements of acidity herein validate the calculations. Future work will focus on probing these acidityselectivity correlations further.

# CONCLUSIONS

Herein we calculate and measure the gas phase acidity of a series of achiral and chiral triazolium precatalysts whose acidities were heretofore unknown. The measurements benchmark the calculations, indicating that the DFT method (B3LYP/6-31+G(d)) is reasonably accurate. Calculations aid in the explanation of surprising trends in gas phase acidity, which are attributable to geometry and the planarity of the N-aryl substituent, relative to the triazolium ring. For the achiral catalysts, the few p $K_a$  values that are known track reasonably well

with the gas phase acidity values, though the acidity range is much tighter in solution than in the gas phase. This wider range of acidities in the gas phase allows for a clear correlation to be tracked between intrinsic acidity values and selectivity in both a homoenolate addition reaction, as catalyzed by achiral triazolylidene catalysts, and a Stetter reaction, as catalyzed by chiral triazolylidene catalysts. These correlations between inherent acidity and selectivity for these types of reactions are the first of their kind, and lead to an improved enantioselectivity in a dienone Stetter reaction. Acidity is shown to be a useful and powerful predictive tool for these types of reactions, and may well extend to other *Umpolung* reactions as well.

## **■ EXPERIMENTAL SECTION**

The synthesis of the protonated carbenes studied herein have been previously described. <sup>4</sup> The reference bases were purchased from Sigma-Aldrich and used as received.

Bracketing experiments were conducted using a house-modified quadrupole ion trap mass spectrometer as previously described. <sup>36</sup> For reactions with reference bases, a reaction efficiency of less than 10% is reported as a "–"; a reaction efficiency of greater than 10% is reported as a "+". <sup>37–39</sup> To generate the protonated carbene ions via electrospray ionization (ESI), the triazolium cations were dissolved in 1:10 water/methanol. About 2  $\mu$ L formic acid was added into every 10 mL water/methanol solution to facilitate ionization. Final concentrations of these solutions were ~10<sup>-4</sup> M.

The flow rates of ESI injection were 15–25  $\mu$ L/min. The capillary temperature was 190 °C. Neutral reference bases were added with

helium gas flow. The protonated carbene ions were allowed to react with neutral reference bases for  $0.03-10\,000$  ms. A total of 10 scans were averaged. The typical electrospray needle voltage was  $\sim 1.80$  kV.

All calculations were performed using density functional theory (B3LYP/6-31+G(d)) as implemented in Gaussian 09.  $^{40-45}$  All the geometries were fully optimized, and frequencies were calculated; no scaling factor was applied. The optimized structures had no negative frequencies. The temperature for the calculations was set to be 298 K. For the enol TS calculations, the SMD model was used with ethanol as the solvent. M06/6-31+G(d,p) solution-phase single-point energy calculations (on the B3LYP/6-31+G(d) geometry) were conducted.  $^{46-50}$  Reported energetics are the sum of the Gibbs free energy correction at B3LYP/6-31+G(d) applied to the solution-phase single-point energy at M06/6-31+G(d,p).

Nitroolefins and nitroesters were both prepared according to previously reported methods:  $^{26}$  A screw-cap vial with a stir-bar was charged with the triazolium salt (0.0125 mmol), NaOAc (5 mg, 0.0625 mmol), and the corresponding nitroolefin, if solid (0.125 mmol); (*E*)-1-nitrobut-1-ene was added immediately before the aldehyde). This vial was then fitted with a rubber septum and evacuated and refilled with nitrogen several times. The vial was then taken into the glovebox, where 0.375 mL (0.33 M relative to nitroalkene) was added, followed by cinnamaldehyde (24.5  $\mu$ L, 0.1875 mmol). The vial was then Teflonlined and allowed to stir at ambient temperature for 16 h. After this time period, 0.125 mmol of trimethoxybenzene was added and the reaction was concentrated via rotary evaporation, taken up in diethyl ether and filtered over a plug of Celite. The diastereomeric ratio was determined according to previously reported HPLC methods and further confirmed through analysis of the  $^{1}$ H NMR spectrum.

Dienones were prepared according to previously reported methods. A flame-dried 20 dram vial was charged with the triazolium salt (0.0122 mmol). The vial was purged under vacuum and refilled with nitrogen three times, and then with 8 mL of anhydrous toluene. Nitrogen was bubbled through the solution for 5 min, and then KHMDS (0.0122 mmol) was added and the solution was allowed to stir at ambient temperature for 10 min. The substrate (0.061 mmol) was dissolved in 0.427 mL of toluene and then dosed via syringe. The reaction was allowed to stir at ambient temperature for 180 min, upon which 1,3,5-trimethoxybenzene (0.061 mmol) was added and the solvent was pumped off and subsequently filtered through a Celite plug with diethyl ether. The enantiomeric excess was determined via separation through a Daicel Chirapak OD-H column with 90:10 hexanes: isopropanol at 1.0 mL/min (major enantiomer: 31.8 min; minor enantiomer: 41.1 min).

### ASSOCIATED CONTENT

# Supporting Information

The Supporting Information is available free of charge on the ACS Publications website at DOI: 10.1021/jacs.7b05229.

Cartesian coordinates for all calculated species and full citations for references with greater than 16 authors (PDF)

# AUTHOR INFORMATION

### **Corresponding Authors**

\*jee.lee@rutgers.edu

\*tr2504@columbia.edu

ORCID

Tomislav Rovis: 0000-0001-6287-8669 Jeehiun K. Lee: 0000-0002-1665-1604

### **Author Contributions**

§Y.N. and N.W. contributed equally to this work.

#### **Notes**

The authors declare no competing financial interest.

### ACKNOWLEDGMENTS

Y.N., N.W., J.X., H.Z., and J.K.L. gratefully thank the NSF and the NSF Extreme Science and Engineering Discovery Environment (XSEDE) for support. T.R. thanks NIGMS (GM72586 for support). A.M. acknowledges NIGMS for a Minority Supplement (GM72586-S1). T.R. thanks Daniel DiRocco (Merck) for the generous gift of aminoindanol.

### REFERENCES

- (1) Igau, A.; Baceiredo, A.; Trinquier, G.; Bertrand, G. Angew. Chem. 1989, 101, 617–618.
- (2) Arduengo, A. J., III; Harlow, R. L.; Kline, M. *J. Am. Chem. Soc.* **1991**, 113, 361–363.
- (3) Samojlowicz, C.; Bieniek, M.; Grela, K. Chem. Rev. 2009, 109, 3708-3742.
- (4) Flanigan, D. M.; Romanov-Michailidis, F.; White, N. A.; Rovis, T. *Chem. Rev.* **2015**, *115*, 9307–9387.
- (5) Enders, D.; Niemeier, O.; Henseler, A. Chem. Rev. 2007, 107, 5606-5655.
- (6) Bugaut, X.; Glorius, F. Chem. Soc. Rev. 2012, 41, 3511-3522.
- (7) Massey, R. S.; Collett, C. J.; Lindsay, A. G.; Smith, A. D.; O'Donoghue, A. C. J. Am. Chem. Soc. **2012**, 134, 20421–20432.
- (8) O'Donoghue, A. C.; Massey, R. S. In *Contemporary Carbene Chemistry*; Moss, R. A., Doyle, M. P., Eds.; Wiley: Hoboken, NJ, 2013; Vol. 7, p 75–106.
- (9) Maji, B.; Breugst, M.; Mayr, H. Angew. Chem., Int. Ed. 2011, 50, 6915-6919.
- (10) Kurinovich, M. A.; Lee, J. K. J. Am. Soc. Mass Spectrom. 2002, 13, 985–995.
- (11) Sun, X.; Lee, J. K. J. Org. Chem. 2007, 72, 6548-6555.
- (12) Liu, M.; Li, T.; Amegayibor, F. S.; Cardoso, D. S.; Fu, Y.; Lee, J. K. J. Org. Chem. **2008**, 73, 9283–9291.
- (13) Michelson, A. Z.; Chen, M.; Wang, K.; Lee, J. K. J. Am. Chem. Soc. **2012**, 134, 9622–9633.
- (14) Liu, M.; Yang, I.; Buckley, B.; Lee, J. K. Org. Lett. **2010**, *12*, 4764–4767.
- (15) Liu, M.; Chen, M.; Zhang, S.; Yang, I.; Buckley, B.; Lee, J. K. J. Phys. Org. Chem. **2011**, 24, 929–936.
- (16) Kaljurand, I.; Koppel, I. A.; Kutt, A.; Rõõm, E.-I.; Rodima, R.; Koppel, I.; Mishima, M.; Leito, I. *J. Phys. Chem. A* **2007**, *111*, 1245–1250.
- (17) A plot of the calculated gas phase acidity versus  $pK_a$  can be found in the Supporting Information.
- (18) Brauman, J. I.; Blair, L. K. J. Am. Chem. Soc. 1970, 92, 5986-5992.
- (19) Ema, T.; Nanjo, Y.; Shiratori, S.; Terao, Y.; Kimura, R. Org. Lett. **2016**, 18, 5764–5767.
- (20) Nair, V.; Sinu, C. R.; Babu, B. P.; Varghese, V.; Jose, A.; Suresh, E. Org. Lett. **2009**, *11*, 5570–5573.
- (21) Maji, B.; Ji, L.; Wang, S.; Vedachalam, S.; Ganguly, R.; Liu, X.-W. *Angew. Chem., Int. Ed.* **2012**, *51*, 8276–8280.
- (22) White, N. A.; DiRocco, D. A.; Rovis, T. J. Am. Chem. Soc. 2013, 135, 8504–8507.
- (23) Plots of selectivity versus calculated acidity for the furyl and phenyl nitroalkenes as well as a plot of selectivity versus experimental acidity for the ethyl nitroalkene are in the Supporting Information.
- (24) H and F are not isosteric. F has an A-value of 0.25 and a van der Waals radius of 1.47 (compared to 1.22 for H).
- (25) (a) Collett, C. J.; Massey, R. S.; Maguire, O. R.; Batsanov, A. S.; O'Donoghue, A. C.; Smith, A. D. Chem. Sci. **2013**, 4, 1514–1522. (b) Zhang, Q.; Yu, H.-Z.; Fu, Y. Org. Chem. Front. **2014**, 1, 614–624.
- (26) Liu, Q.; Rovis, T. J. Am. Chem. Soc. 2006, 128, 2552-2553.
- (27) For precatalysts 2a, 2b, 2d, 2e, and 2h, the enantiomers were utilized for the ee experiments; however, the gas phase acidity is still relevant since this value remains the same regardless of enantiomer.
- (28) Liu, Q.; Rovis, T. Org. Process Res. Dev. 2007, 11, 598-604.
- (29) Kim, Y.-J.; Streitwieser, A. J. Am. Chem. Soc. 2002, 124, 5757–5761.

- (30) Sievers, A.; Wolfenden, R. J. Am. Chem. Soc. 2002, 124, 13986–3987
- (31) Washabaugh, M. W.; Jencks, W. P. J. Am. Chem. Soc. 1989, 111, 674–683.
- (32) Alder, R. W.; Allen, P. R.; Williams, S. J. J. Chem. Soc., Chem. Commun. 1995, 1267–1268.
- (33) Chu, Y.; Deng, H.; Cheng, J.-P. J. Org. Chem. 2007, 72, 7790-7793.
- (34) Amyes, T. L.; Diver, S. T.; Richard, J. P.; Rivas, F. M.; Toth, K. J. Am. Chem. Soc. **2004**, 126, 4366–4374.
- (35) Higgins, E. M.; Sherwood, J. A.; Lindsay, A. G.; Armstrong, J.; Massey, R. S.; Alder, R. W.; O'Donoghue, A. C. *Chem. Commun.* **2011**, 47, 1559–1562.
- (36) Liu, M.; Chen, M.; Zhang, S.; Yang, I.; Buckley, B.; Lee, J. K. J. Phys. Org. Chem. 2011, 24, 929–936.
- (37) Chesnavich, W. J.; Su, T.; Bowers, M. T. J. Chem. Phys. 1980, 72, 2641–2655.
- (38) Su, T.; Chesnavich, W. J. J. Chem. Phys. 1982, 76, 5183-5185.
- (39) Miller, K. J.; Savchik, J. A. J. Am. Chem. Soc. **1979**, 101, 7206–7213.
- (40) Lee, C.; Yang, W.; Parr, R. G. Phys. Rev. B: Condens. Matter Mater. Phys. 1988, 37, 785–789.
- (41) Becke, A. D. J. Chem. Phys. 1993, 98, 5648-5652.
- (42) Becke, A. D. J. Chem. Phys. 1993, 98, 1372-1377.
- (43) Stephens, P. J.; Devlin, F. J.; Chabalowski, C. F.; Frisch, M. J. J. Phys. Chem. **1994**, 98, 11623–11627.
- (44) Kohn, W.; Becke, A. D.; Parr, R. G. J. Phys. Chem. 1996, 100, 12974–12980.
- (45) Frisch, M. J.; Trucks, G. W.; Schlegel, H. B.; Scuseria, G. E.; Robb, M. A.; Cheeseman, J. R.; Scalmani, G.; Barone, V.; Mennucci, B.; Petersson, G. A.; Nakatsuji, H.; Caricato, M.; Li, X.; Hratchian, H. P.; Izmaylov, A. F.; Bloino, J.; Zheng, G.; Sonnenberg, J. L.; Hada, M.; Ehara, M.; Toyota, K.; Fukuda, R.; Hasegawa, J.; Ishida, M.; Nakajima, T.; Honda, Y.; Kitao, O.; Nakai, H.; Vreven, T.; Montgomery, J. J. A.; Peralta, J. E.; Ogliaro, F.; Bearpark, M.; Heyd, J. J.; Brothers, E.; Kudin, K. N.; Staroverov, V. N.; Kobayashi, R.; Normand, J.; Raghavachari, K.; Rendell, A.; Burant, J. C.; Iyengar, S. S.; Tomasi, J.; Cossi, M.; Rega, N.; Millam, J. M.; Klene, M.; Knox, J. E.; Cross, J. B.; Bakken, V.; Adamo, C.; Jaramillo, J.; Gomperts, R.; Stratmann, R. E.; Yazyev, O.; Austin, A. J.; Cammi, R.; Pomelli, C.; Ochterski, J. W.; Martin, R. L.; Morokuma, K.; Zakrzewski, V. G.; Voth, G. A.; Salvador, P.; Dannenberg, J. J.; Dapprich, S.; Daniels, A. D.; Farkas, Ö.; Foresman, J. B.; Ortiz, J. V.; Cioslowski, J.; Fox, D. J. GAUSSIAN09, rev. A.; Gaussian, Inc.: Wallingford, C.T., 2009.
- (46) Marenich, A. V.; Cramer, C. J.; Truhlar, D. G. J. Phys. Chem. B **2009**, 113, 6378–6396.
- (47) Miertuš, S.; Scrocco, E.; Tomasi, J. Chem. Phys. 1981, 55, 117–129.
- (48) Pascual-Ahuir, J. L.; Silla, E.; Tuñon, I. J. Comput. Chem. 1994, 15, 1127–1138.
- (49) Zhao, Y.; Truhlar, D. G. Theor. Chem. Acc. 2008, 120, 215-241.
- (50) Zhao, Y.; Truhlar, D. G. Acc. Chem. Res. 2008, 41, 157-167.